CHULA ENGINEERING
Innovation toward Sustainability | ACTNOW

MICROWAVE REMOTE SENSING

Geospatial Programming

Modern Integrated Surveying Technologies 2023

Thepchai Srinoi

Graduate Student and Teaching Assistant,

Department of Survey Engineering Chulalongkorn University

Atmospheric Windows – Welcome to RADAR

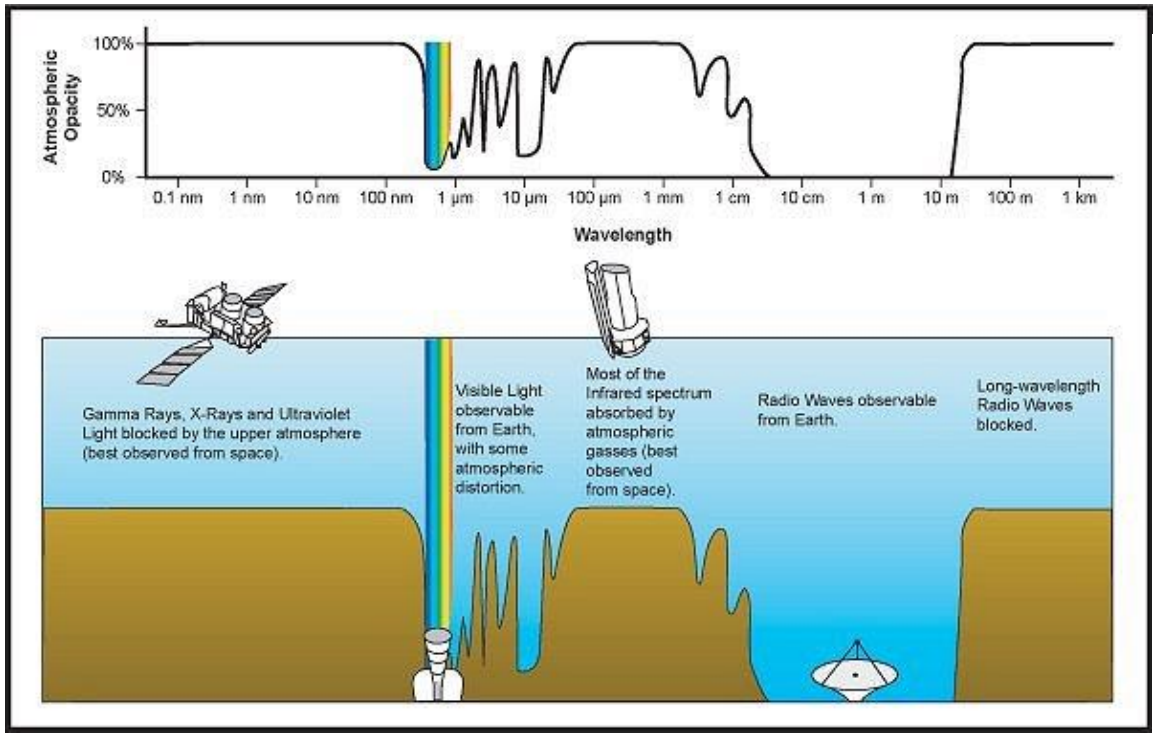

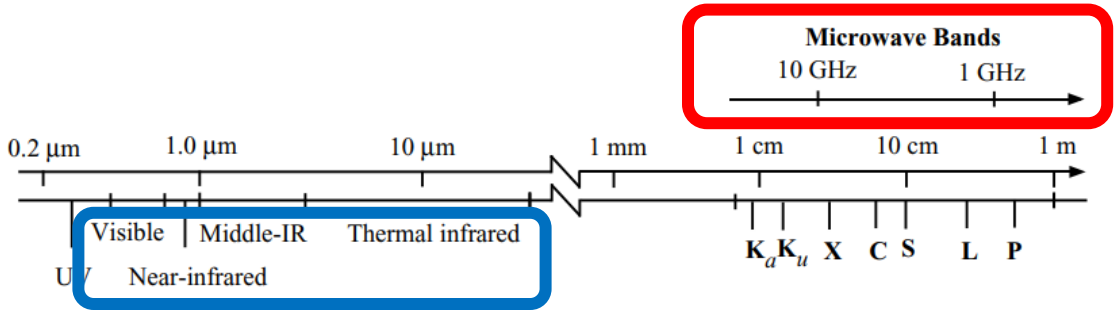

Table 2. Advantages of RADAR remote sensing.

Advantages
Primary
• Certain microwave frequencies will penetrate clouds, allowing all-weather remote sensing.
• Synoptic views of large areas for mapping at 1:10,000 to 1:400,000. Satellite coverage of cloud-shrouded countries is possible.
• Coverage can be obtained at user-specified times, even at night.
• Permits imaging at shallow look angles, resulting in different perspectives that cannot always be obtained using aerial photography.
• Senses in wavelengths outside the visible and infrared regions of the electromagnetic spectrum, providing information on surface roughness, dielectric properties, and moisture content.
Secondary
• Certain frequencies of microwave energy penetrate vegetation, sand, and surface layers of snow.
• Based on its own illumination, and the angle of illumination can be controlled.
• Enables resolution to be independent of distance to the object, with the size of a resolution cell being as small as 1 × 1 m.
• Images can be produced from different types of polarized energy (HH, HV, VV, VH).
• May operate simultaneously in several wavelengths (frequencies) and thus has multi-frequency potential.
• Can measure ocean wave properties, even from orbital altitudes.
• Can produce overlapping images suitable for stereoscopic viewing and radargrammetry.
• Supports interferometric operation using two antennas for 3-D mapping, and analysis of incident-angle signatures of objects.

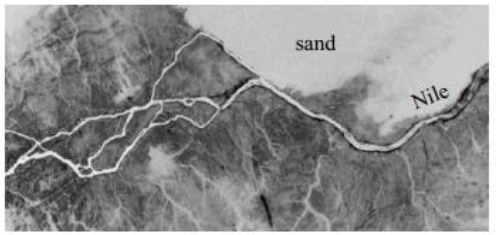

a. Shuttle photograph.

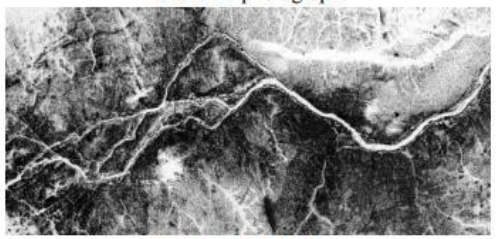
b. SIR-C C-band HV.


c. SIR-C L-band HV.


d. SIR-C L-band HH.

Passive and Active Remote Sensing

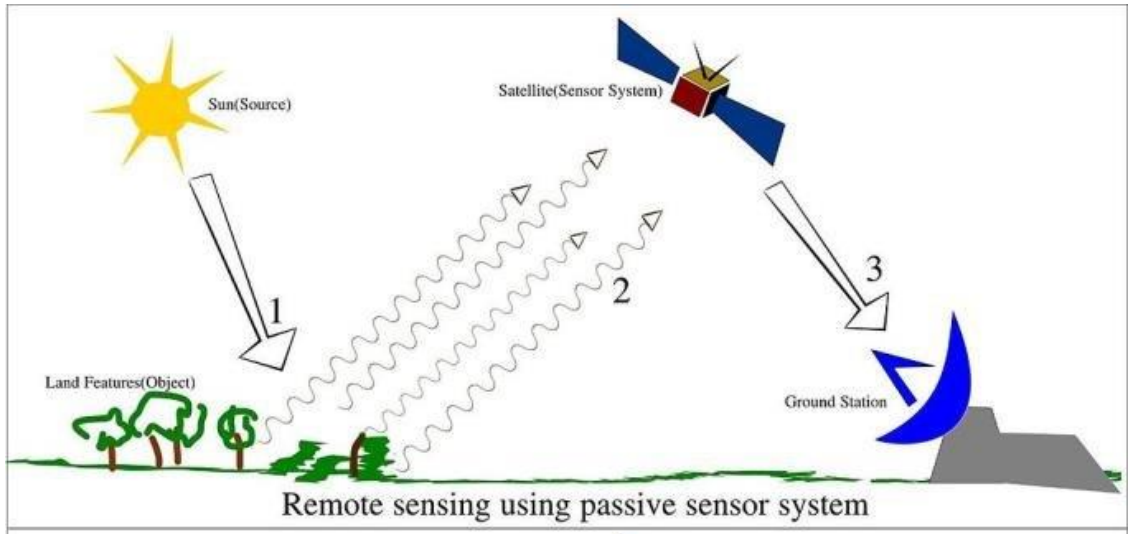

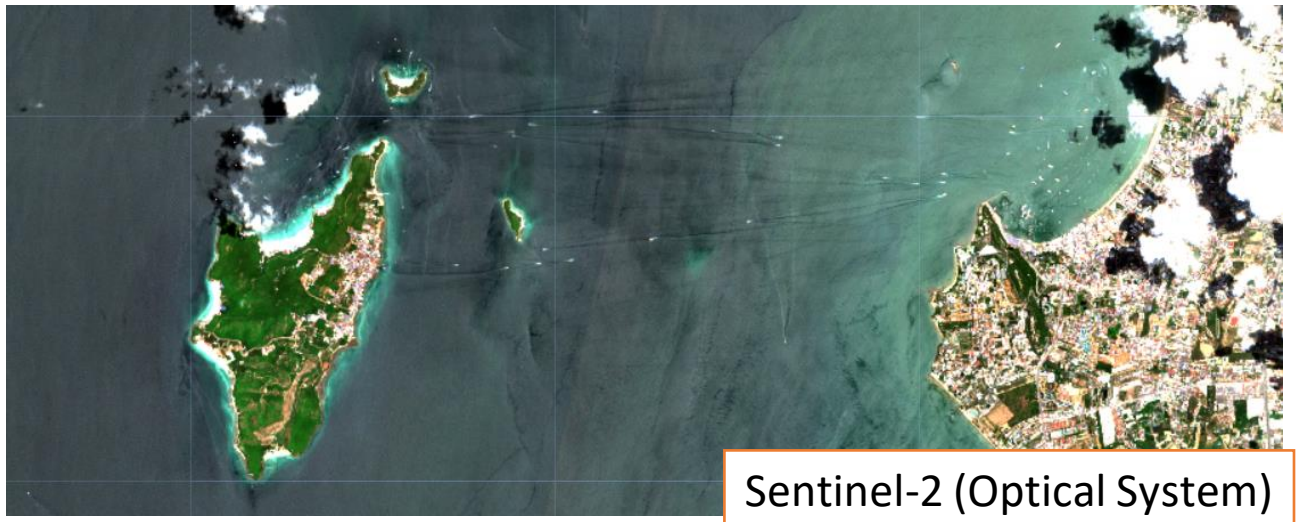

Sentinel-2 (Optical System)

Sentinel-1 (SAR System)

RADAR – Radio Detection and Ranging

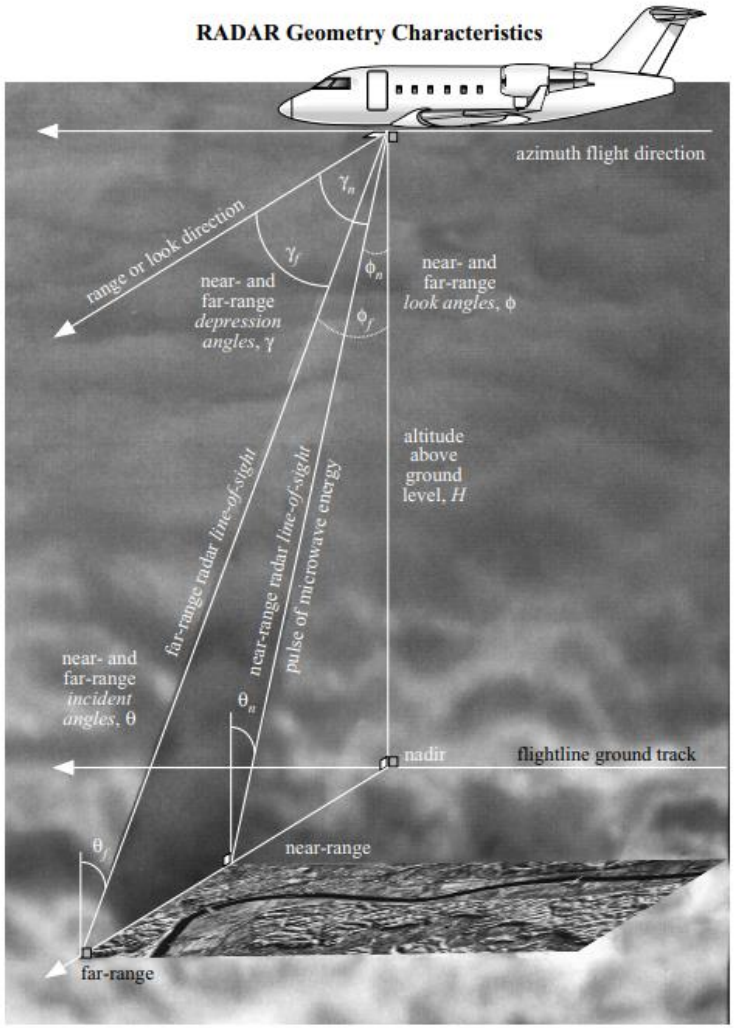

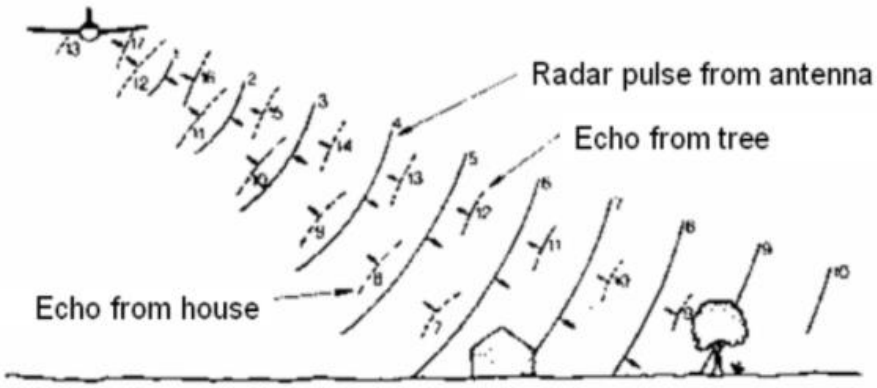

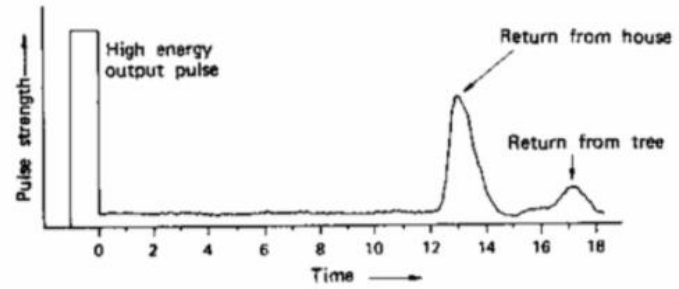

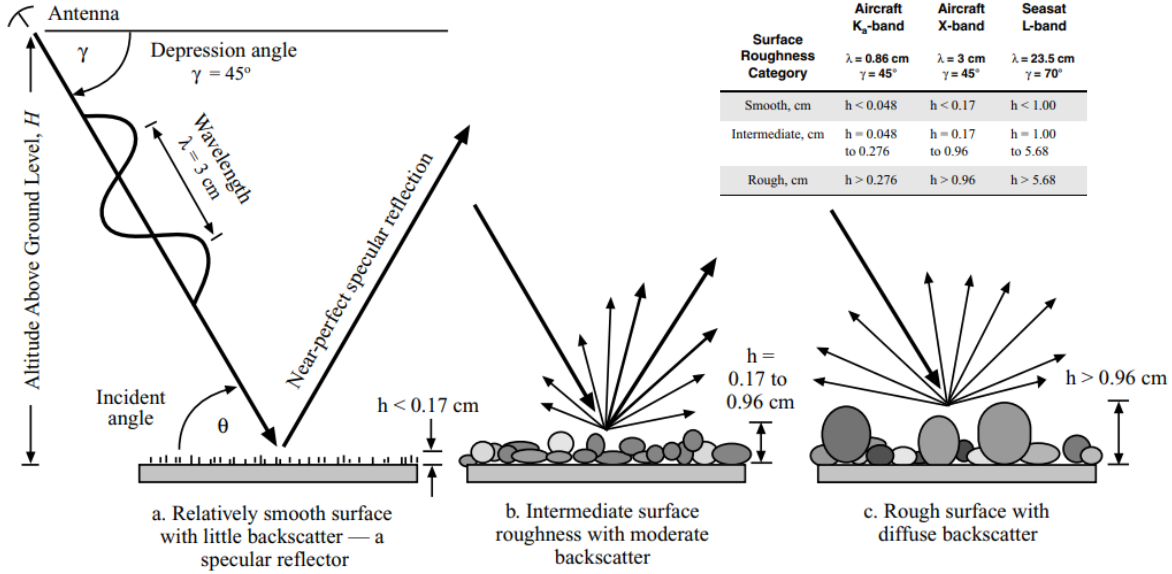

Surface Roughness Category	Aircraft K_a-band λ = 0.86 cm γ = 45°	Aircraft X-band λ = 3 cm γ = 45°	Seasat L-band λ = 23.5 cm γ = 70°
Smooth, cm	h < 0.048	h < 0.17	h < 1.00
Intermediate, cm	h = 0.048 to 0.276	h = 0.17 to 0.96	h = 1.00 to 5.68
Rough, cm	h > 0.276	h > 0.96	h > 5.68

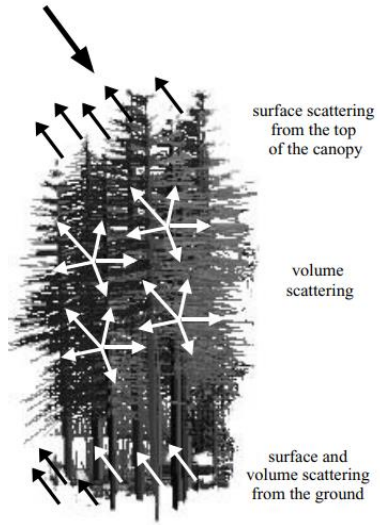

Doppler principles are then used to monitor the returns from all these additional microwave pulses to synthesize the azimuth resolution to become one very narrow beam.

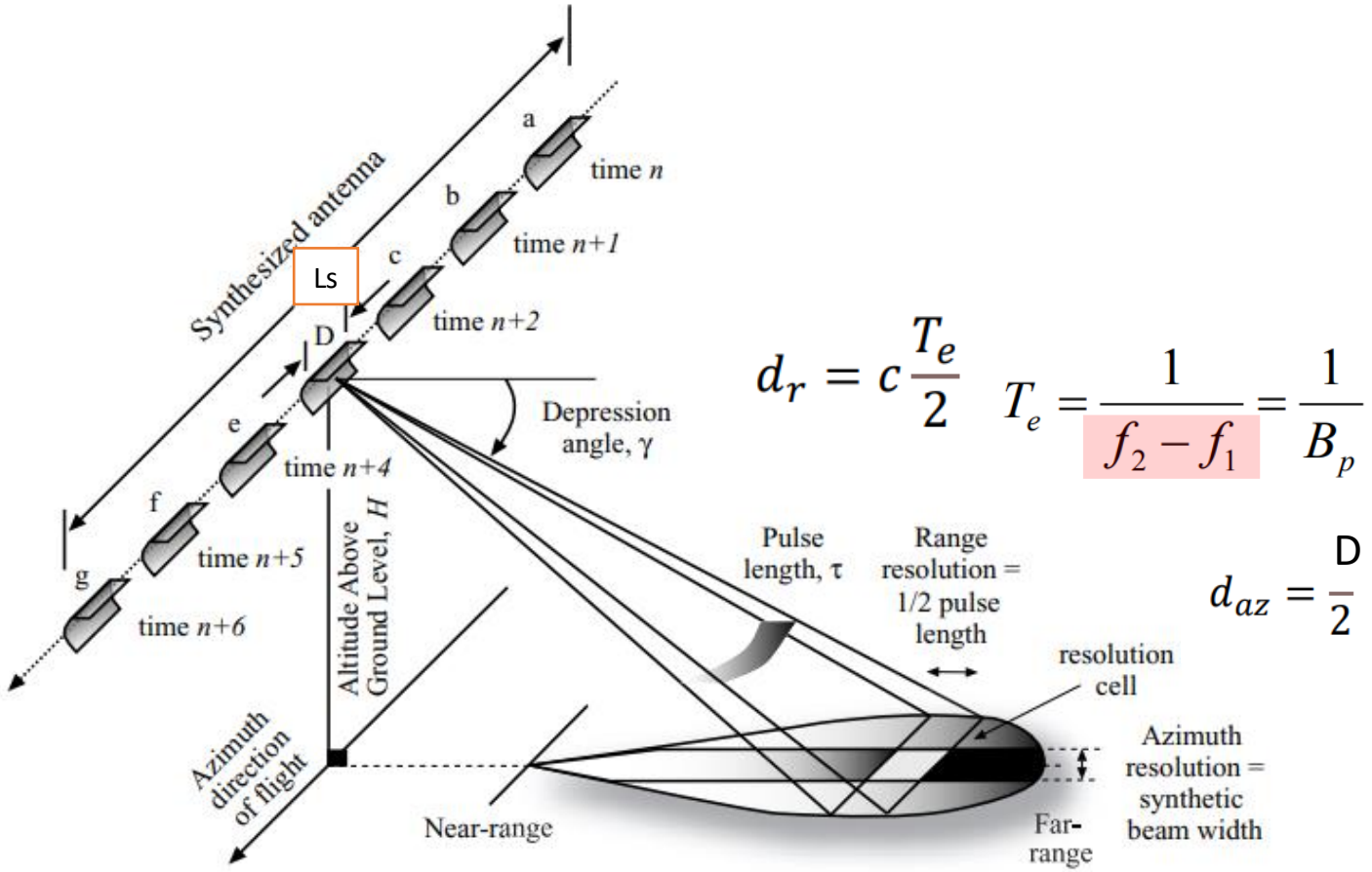

$$d_r = c\frac{T_e}{2} \qquad T_e = \frac{1}{f_2 - f_1} = \frac{1}{B_p}$$

$$d_{az} = \frac{D}{2}$$

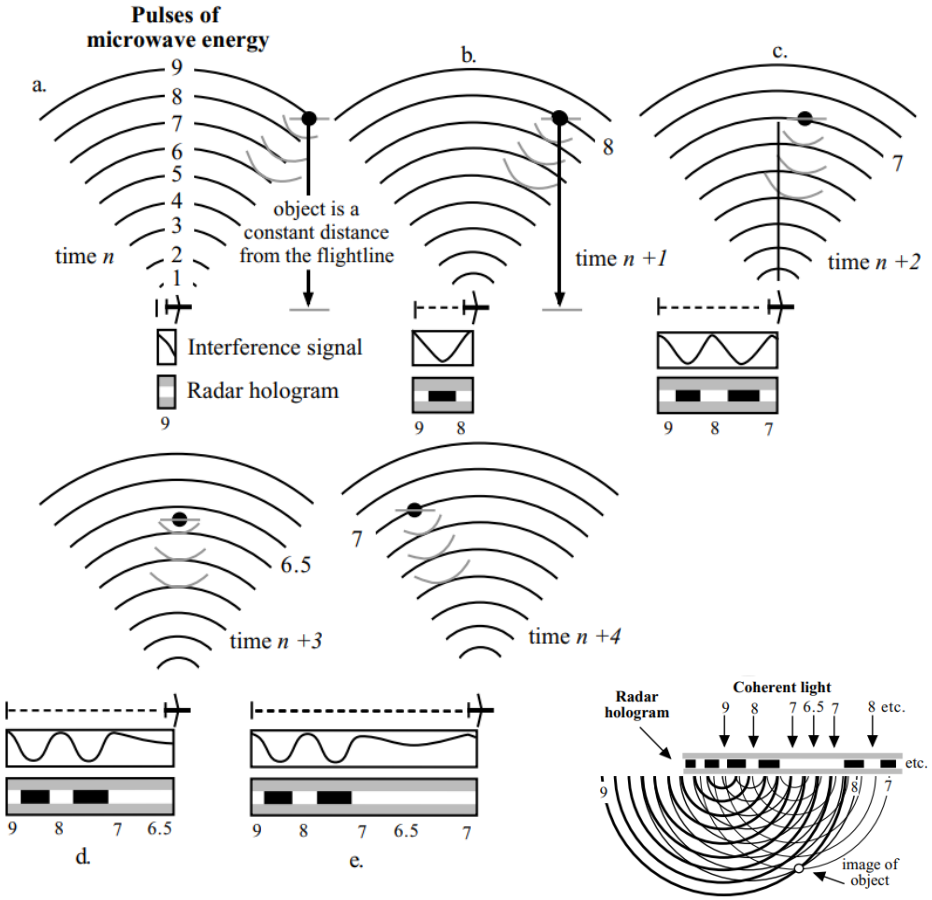

Orbital Direction and Geometric Distortion

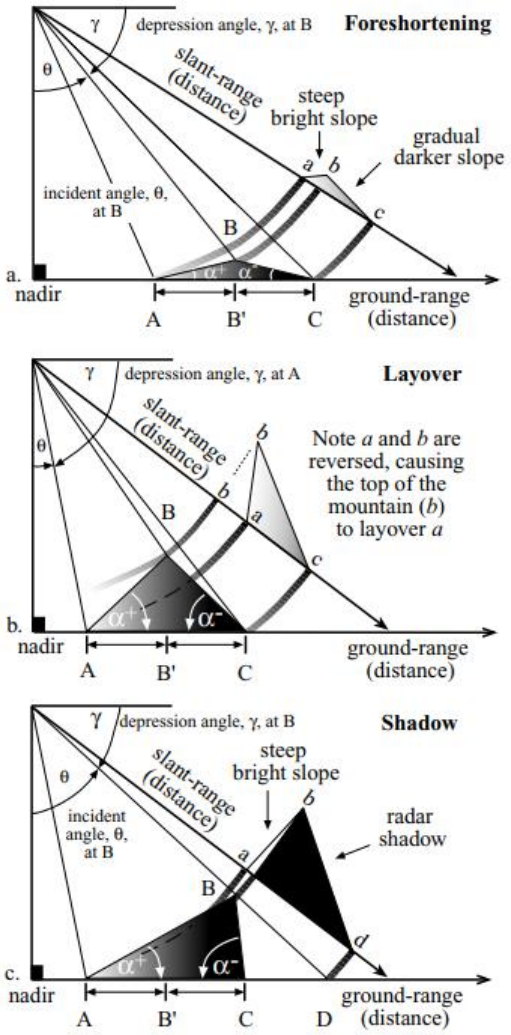

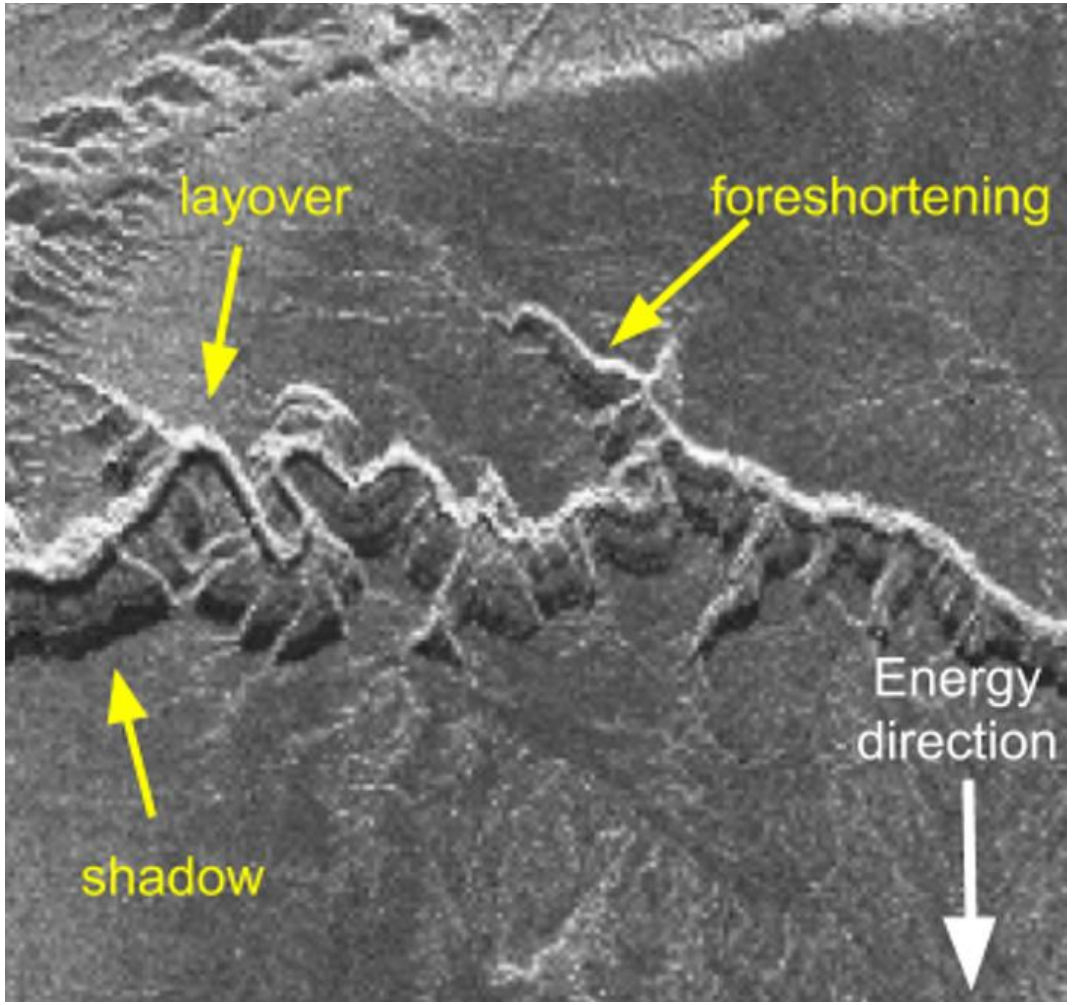

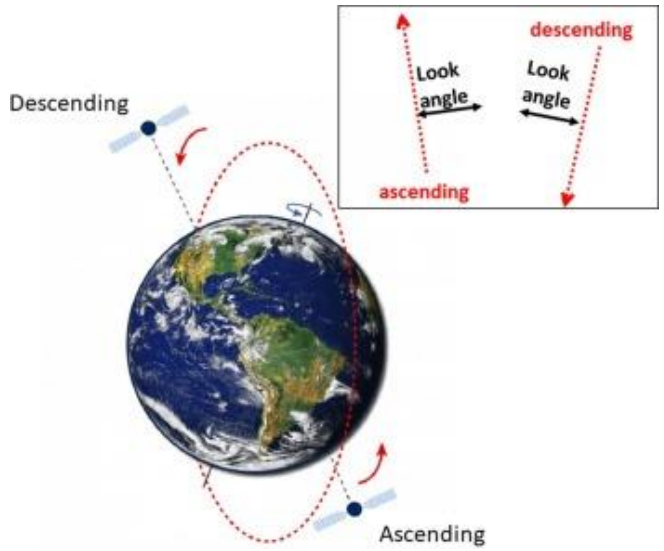

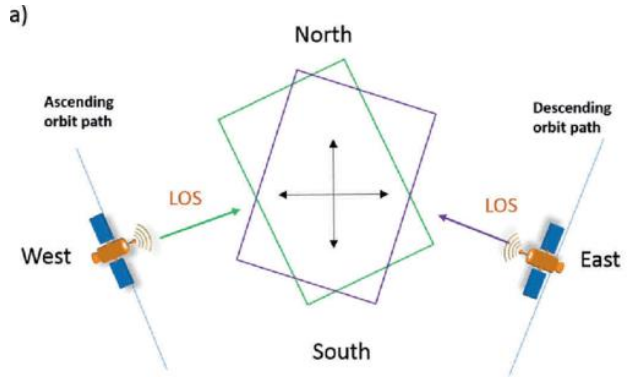

SAR Polarization

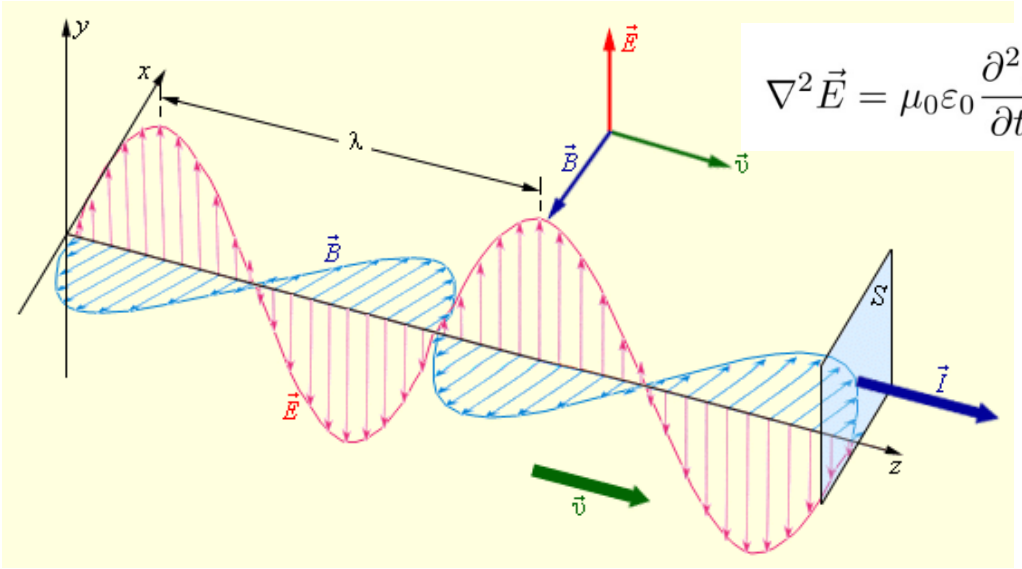

$$\nabla^2 \vec{E} = \mu_0 \varepsilon_0 \frac{\partial^2 \vec{E}}{\partial t^2} \qquad \nabla^2 \vec{B} = \mu_0 \varepsilon_0 \frac{\partial^2 \vec{B}}{\partial t^2}$$

$$\vec{S} = \frac{1}{\mu_0} \vec{E} \times \vec{B}$$

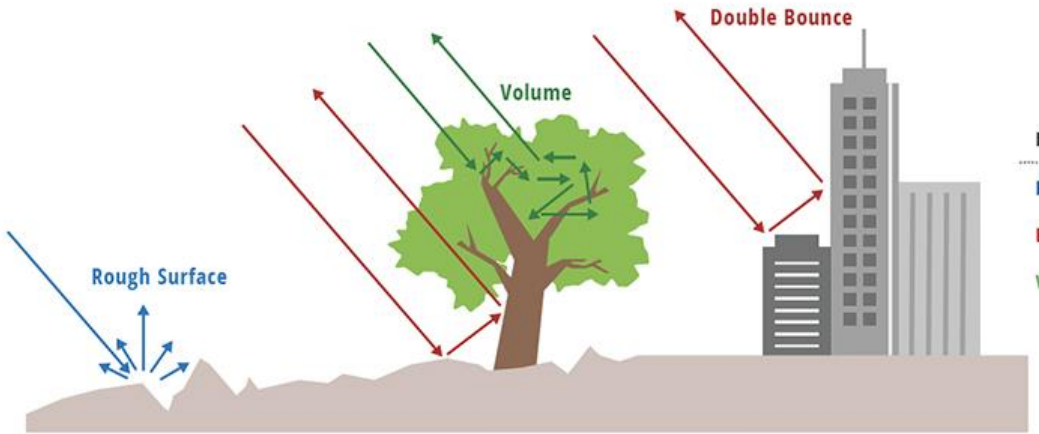

RELATIVE SCATTERING STRENGTH BY POLARIZATION:

Rough Surface Scattering	$\|S_{VV}\| > \|S_{HH}\| > \|S_{HV}\|$ or $\|S_{VH}\|$
Double Bounce Scattering	$\|S_{HH}\| > \|S_{VV}\| > \|S_{HV}\|$ or $\|S_{VH}\|$
Volume Scattering	Main source of $\|S_{HV}\|$ and $\|S_{VH}\|$

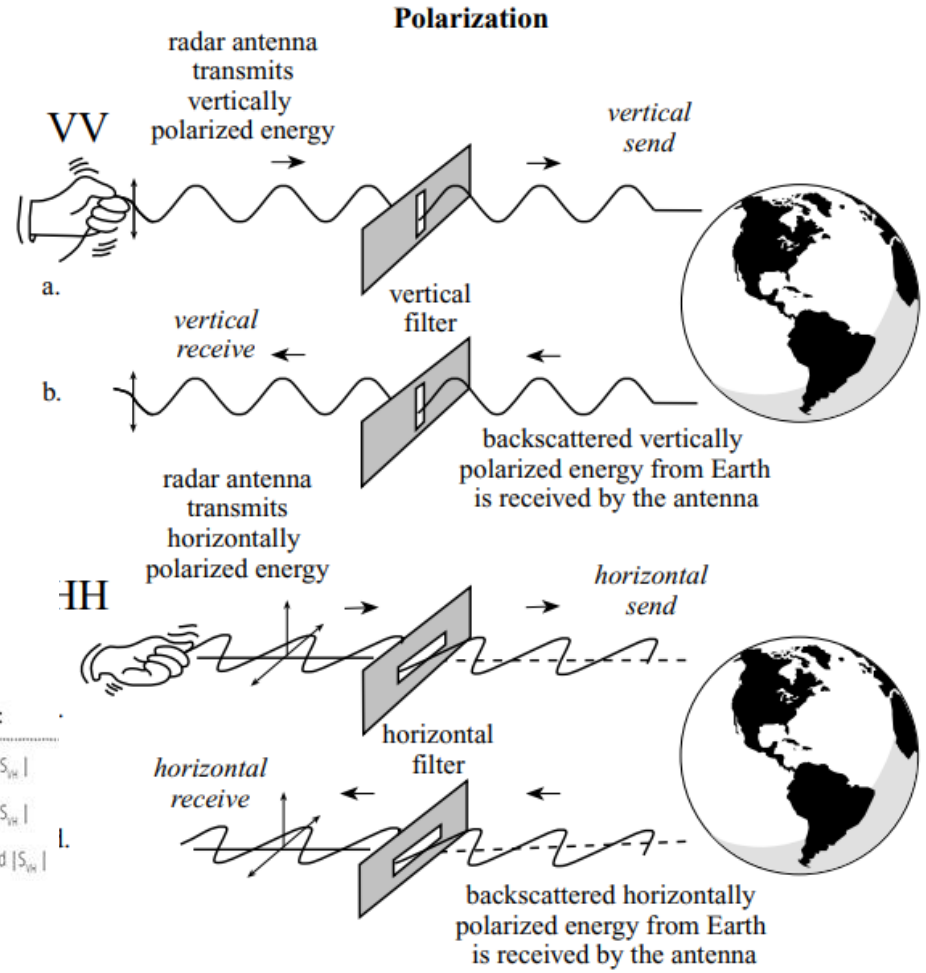

SAR Product

A heavy rain in the lower center of the image appears as a black “cloud” in the X-band image, more faintly in the C-band image, and is invisible in the L-band image.

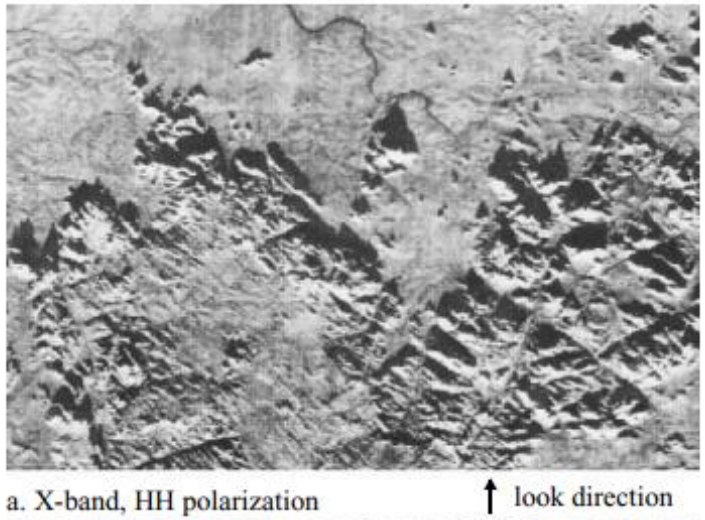

a. X-band, HH polarization ↑ look direction

b. X-band, HH polarization ↓ look direction

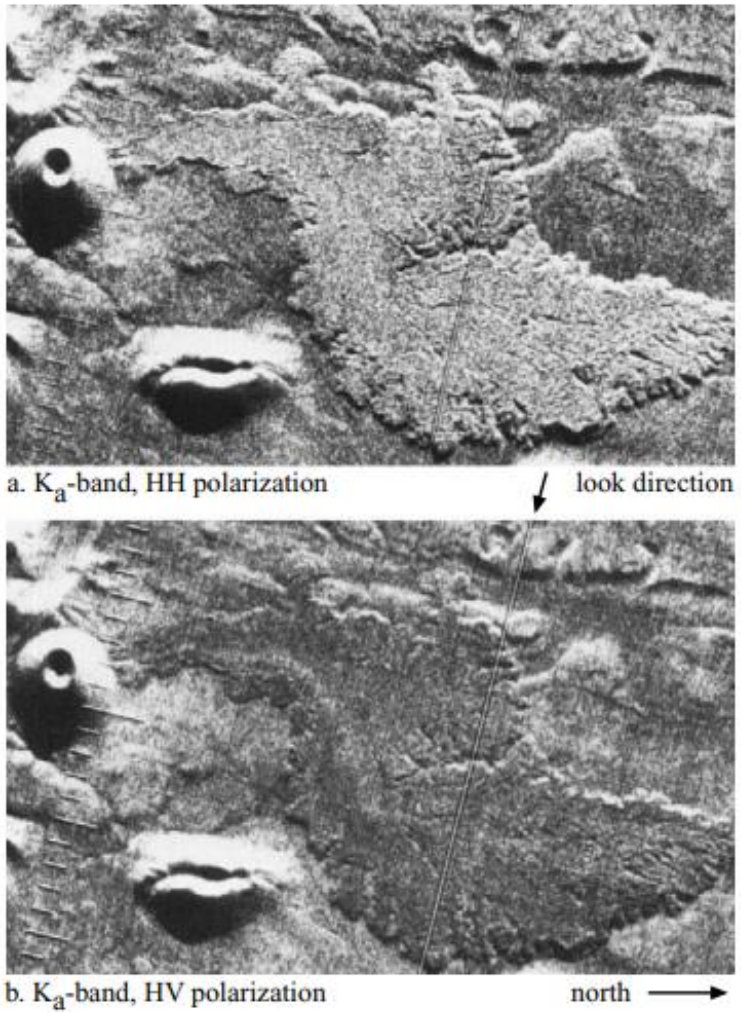

a. K_a-band, HH polarization ↓ look direction

b. K_a-band, HV polarization → north

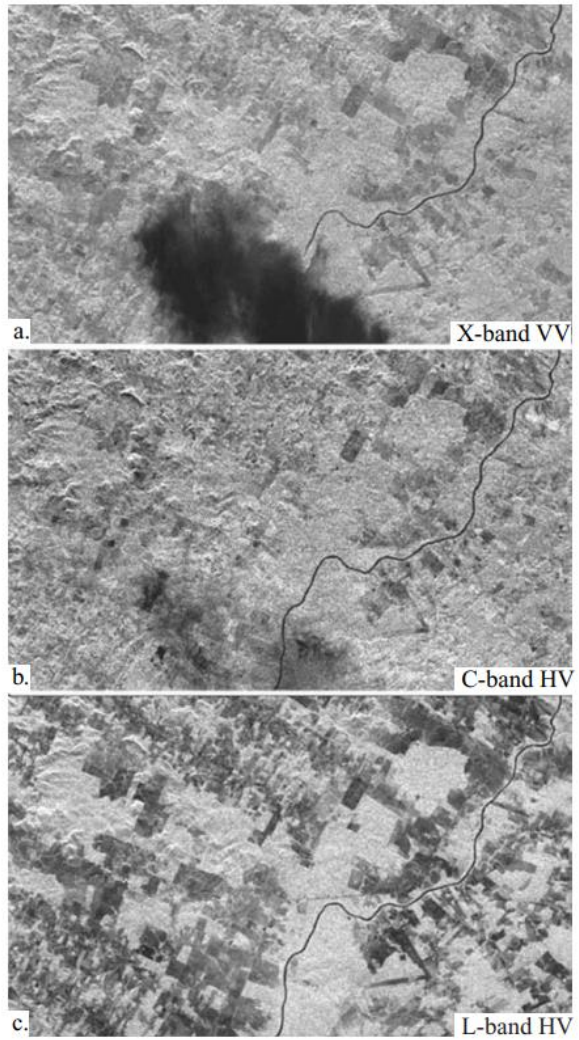

SAR Product - Polarimetry

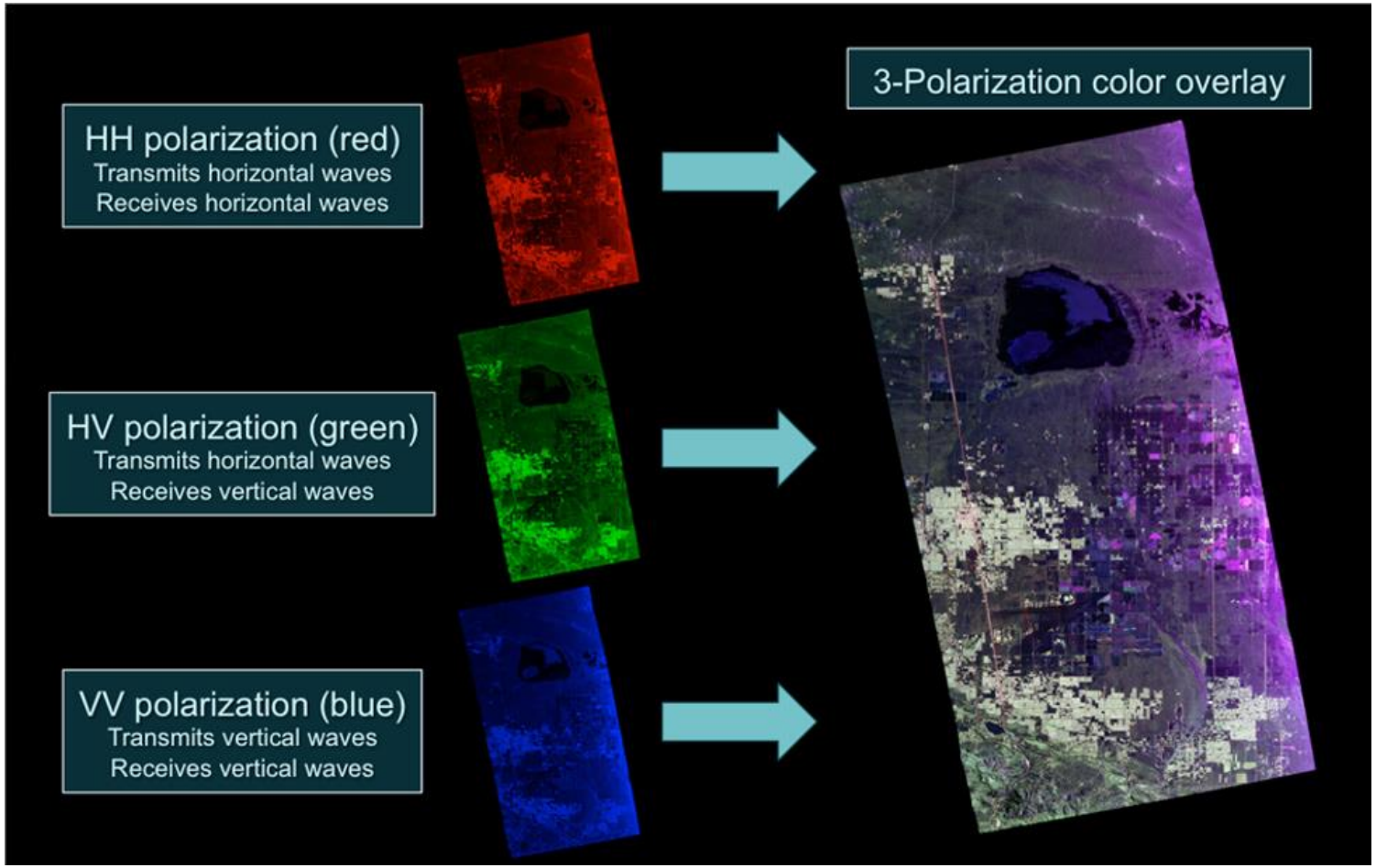

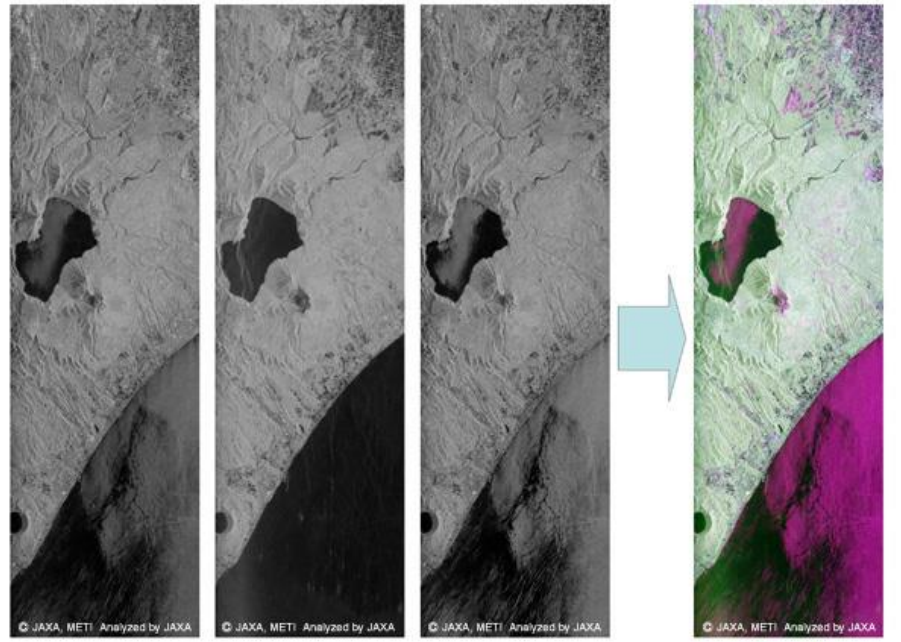

2006/08/19 01:17(UT) ALOS/PALSAR POLARIMETRY

Selected Airport feature-A and feature B (Location 7 & 8)

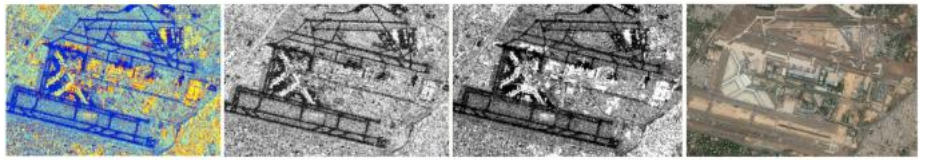

(a) (R: VV, G: VH, B: VH/VV) *VH Polarisation* *VV Polarisation* *Google Image*-**Airport-A**

SAR Product – Object Detection

Container terminals

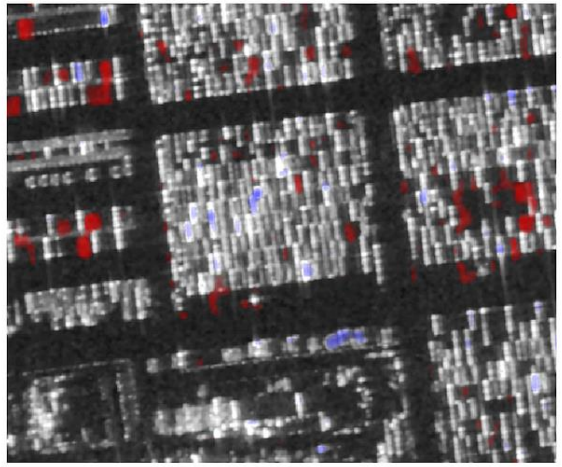

Ship arrived to oil terminal

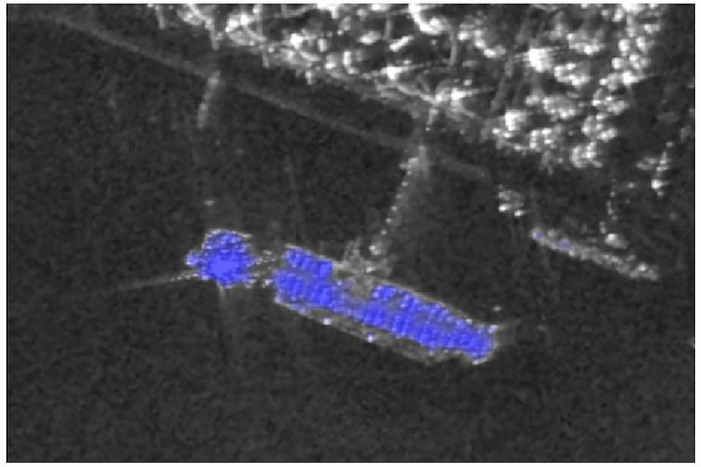

Movement of trains, coal transport

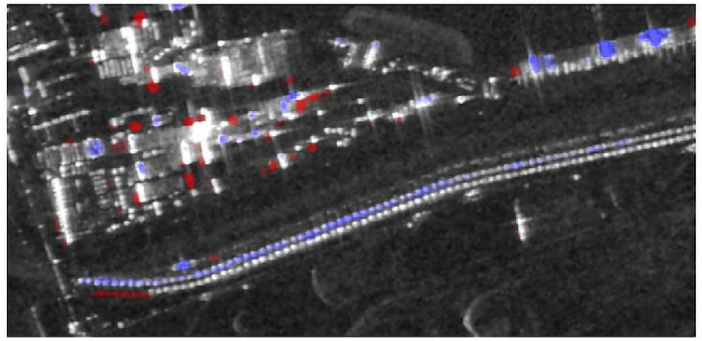

Floating roof oil tanks

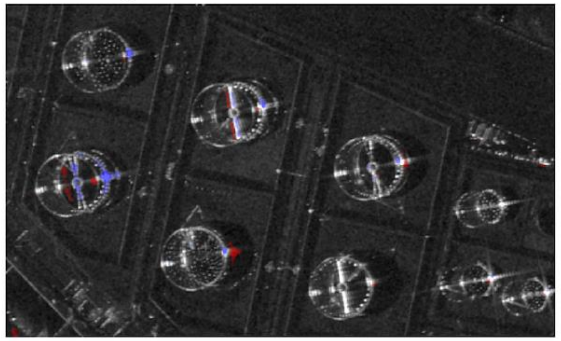

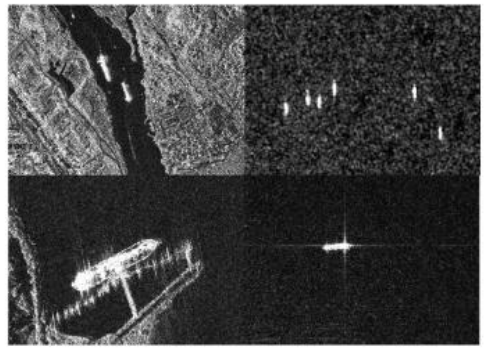

Exploiting automated change detection on Persistent Monitoring high-resolution Imagery

SAR Product – Crop and Flood Monitoring

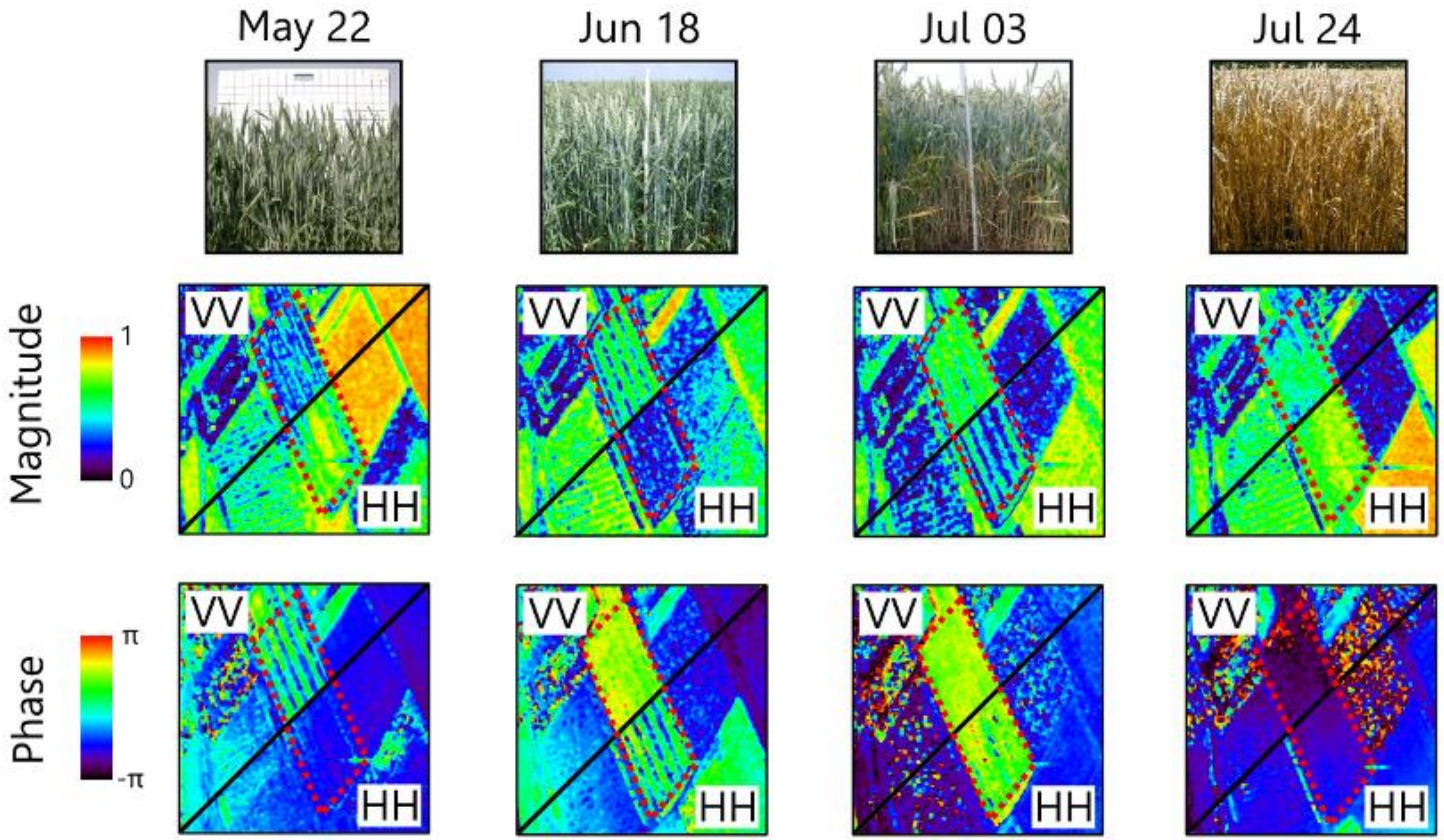

SAR Polarimeteric analysis of agricultural crops. Magnitude (above) and phase (below) of the interferometric coherence for a wheat field throughout the plant growth season.

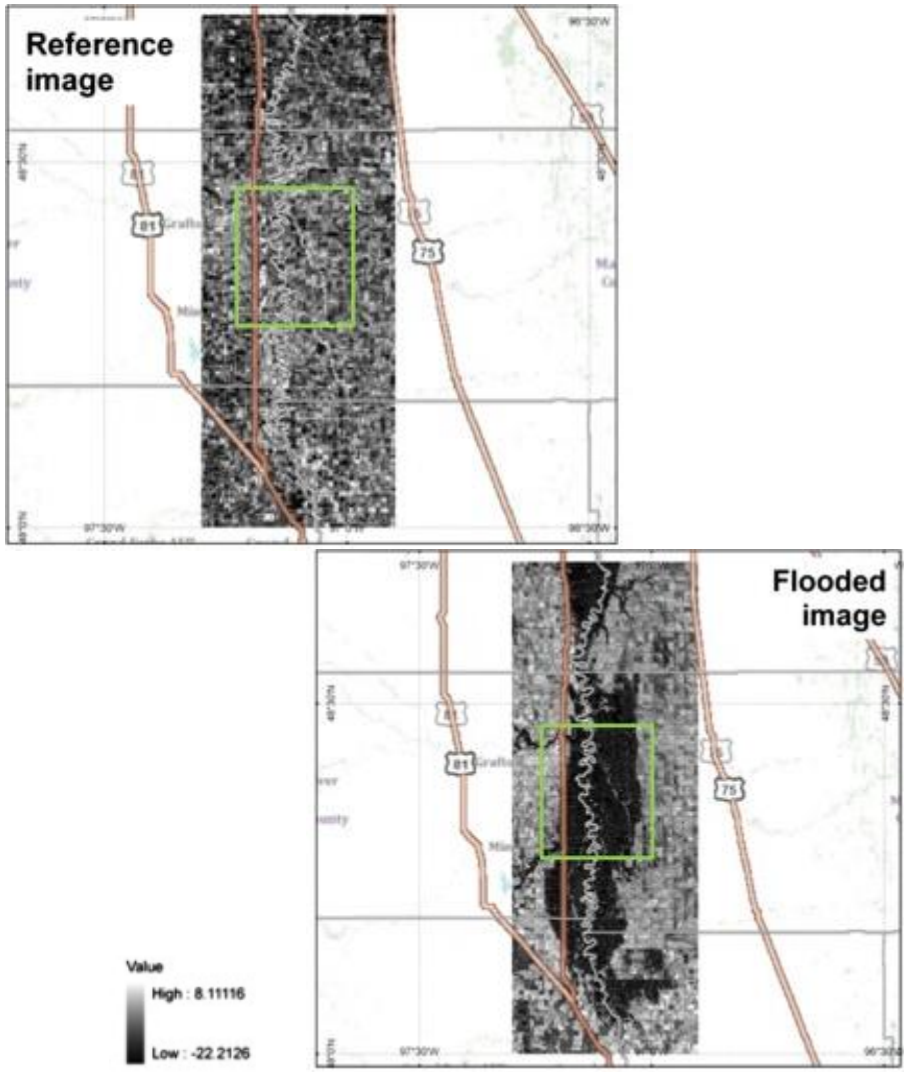

Input : Optical + SAR image

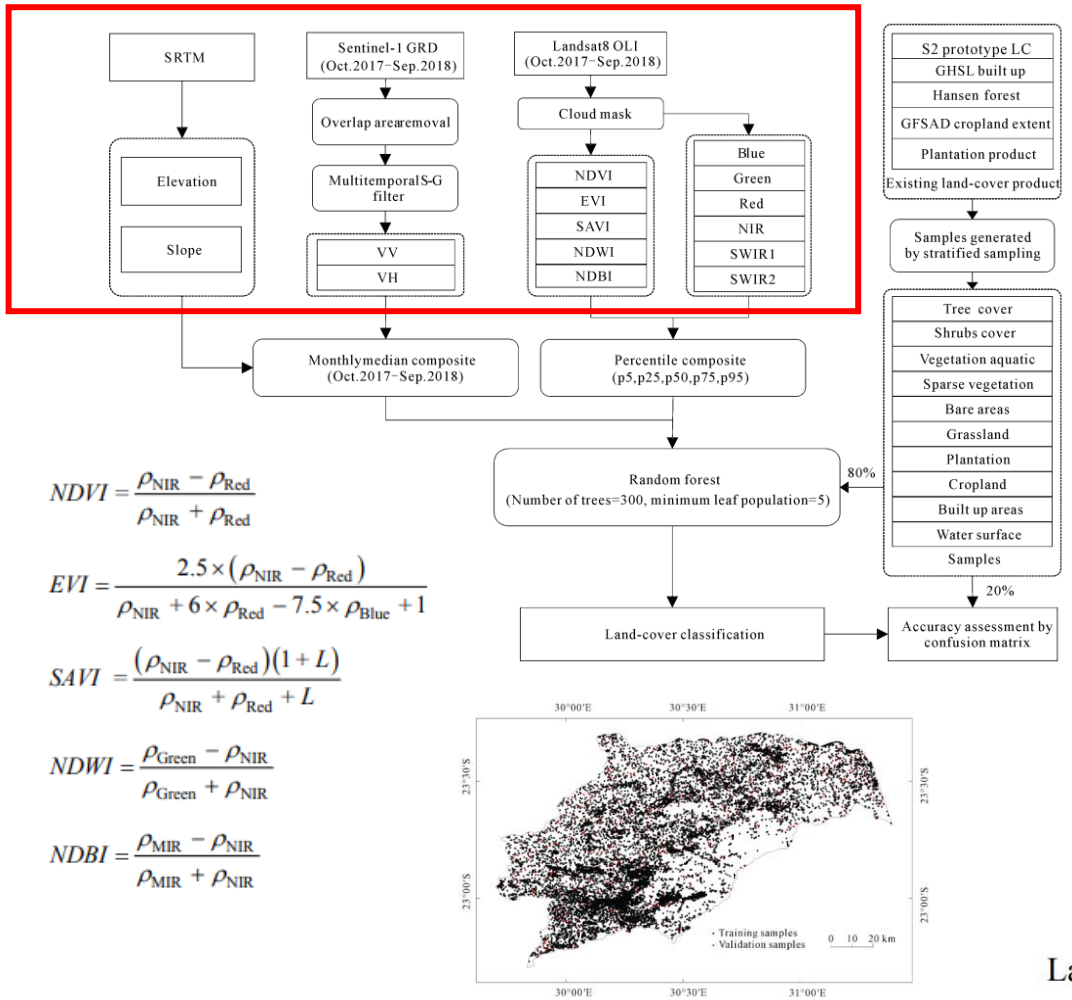

$$NDVI = \frac{\rho_{NIR} - \rho_{Red}}{\rho_{NIR} + \rho_{Red}}$$

$$EVI = \frac{2.5 \times (\rho_{NIR} - \rho_{Red})}{\rho_{NIR} + 6 \times \rho_{Red} - 7.5 \times \rho_{Blue} + 1}$$

$$SAVI = \frac{(\rho_{NIR} - \rho_{Red})(1 + L)}{\rho_{NIR} + \rho_{Red} + L}$$

$$NDWI = \frac{\rho_{Green} - \rho_{NIR}}{\rho_{Green} + \rho_{NIR}}$$

$$NDBI = \frac{\rho_{MIR} - \rho_{NIR}}{\rho_{MIR} + \rho_{NIR}}$$

A Synthesizing Land-cover Classification Method Based on Google Earth Engine: A Case Study in Nzhelele and Levhuvu Catchments, South Africa

https://doi.org/10.1007/s11769-020-1119-y

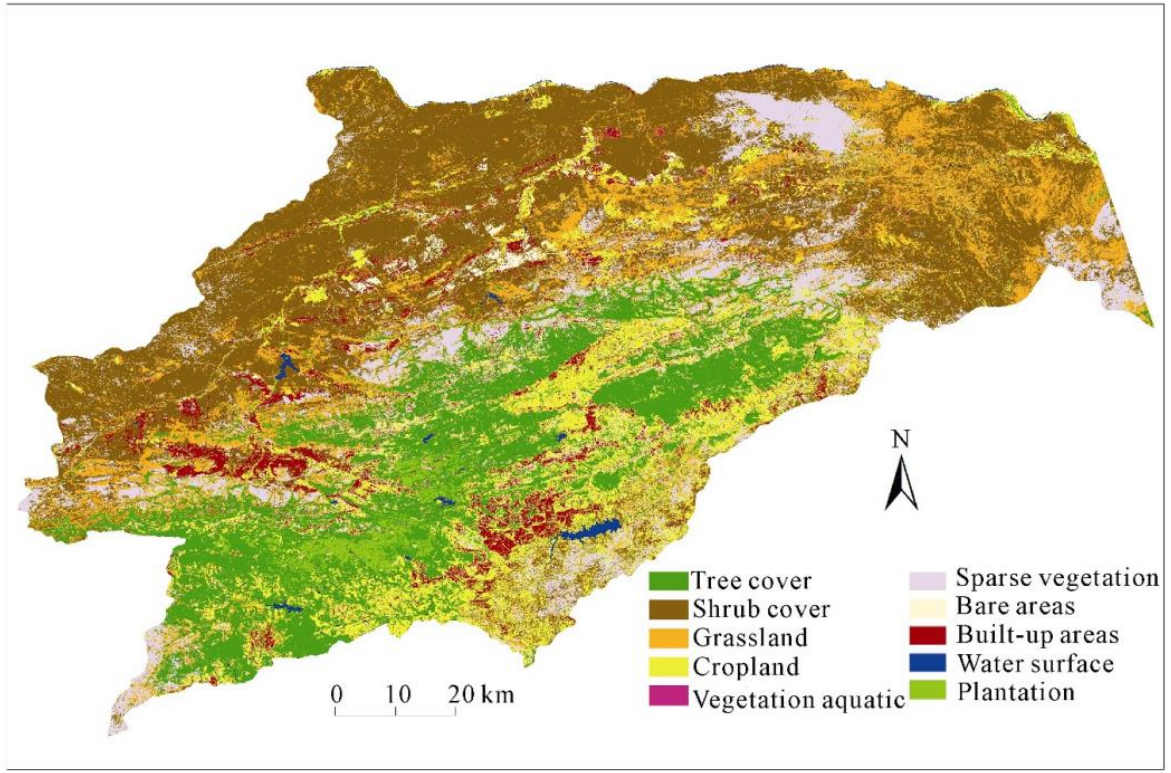

Land-cover map of Nzhelele and Levhuvu catchments, South Africa in 2017–2018

Optical + SAR Research – Height Estimation

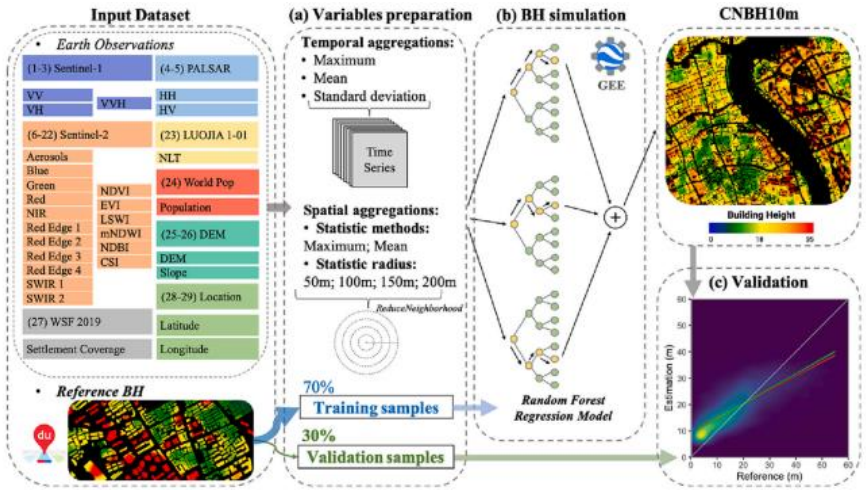

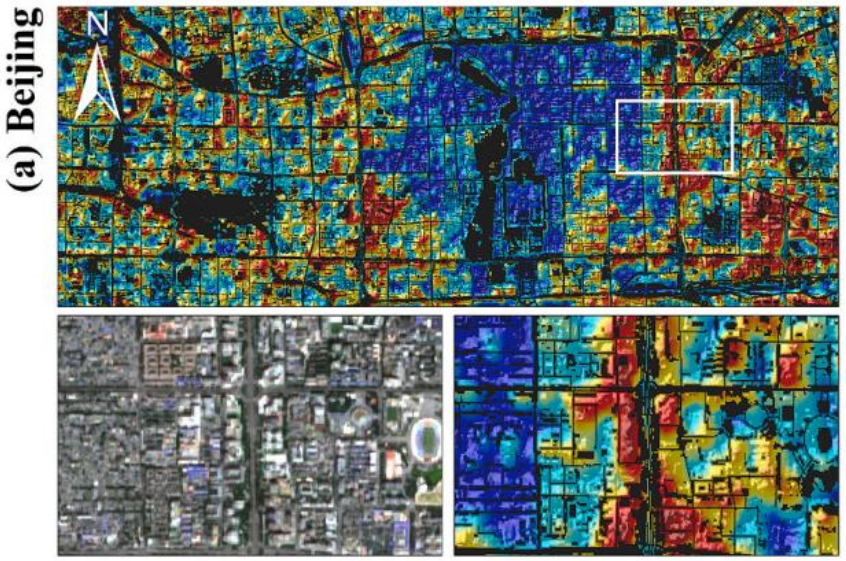

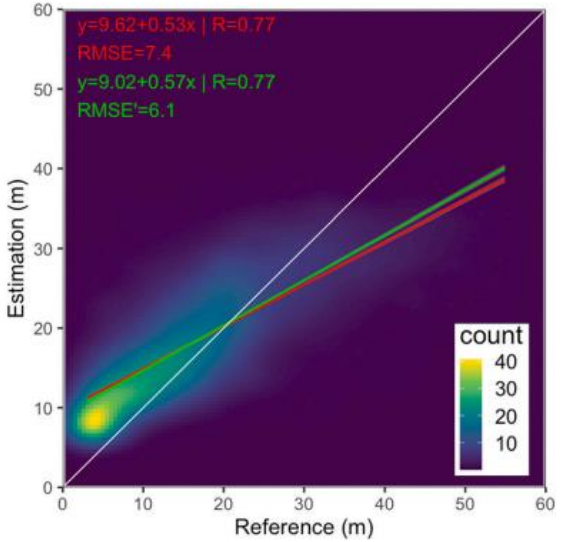

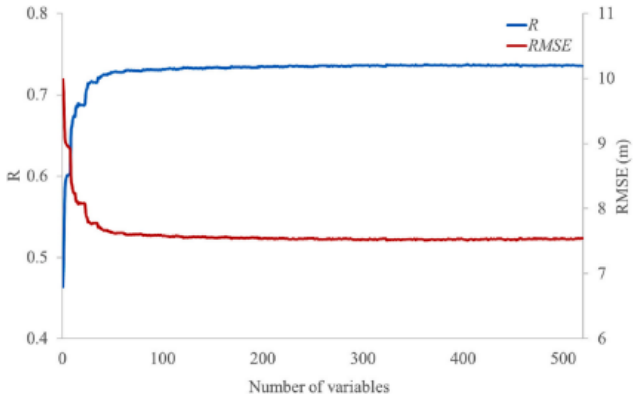

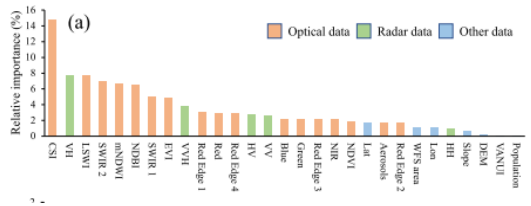

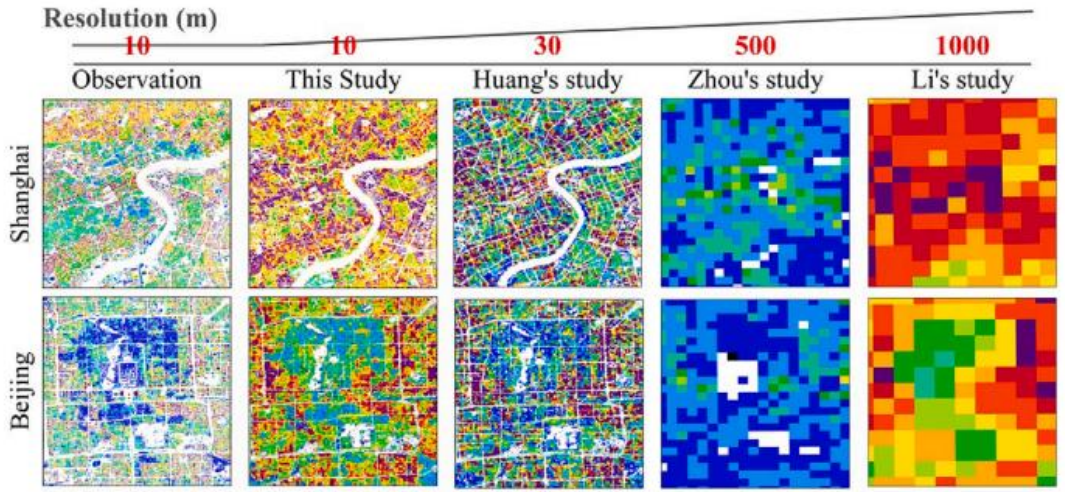

A first Chinese building height estimate at 10 m resolution (CNBH-10 m) using multi-source earth observations and machine learning (Wan-Ben Wu et al, 2023)

THE END ....

Geospatial Programming

Modern Integrated Surveying Technologies 2024

Thepchai Srinoi

Master Degree Student and Teaching Assistant,

Department of Survey Engineering Chulalongkorn University